Probabilistic Mapping of Stability and Reliability in Microgrids – A Bayesian Interpretation

Song, Yubo; Sahoo, Subham; Yang, Yongheng; Blaabjerg, Frede

Published in:
2023 25th European Conference on Power Electronics and Applications (EPE'23 ECCE Europe)

DOI (link to publication from Publisher):
10.23919/EPE23ECCEEurope58414.2023.10264295

Publication date:
2023

Document Version
Accepted author manuscript, peer reviewed version

Probabilistic Mapping of Stability and Reliability in Microgrids – A Bayesian Interpretation

Yubo Song[1], Subham Sahoo[1], Yongheng Yang[2], and Frede Blaabjerg[1]

[1] Department of Energy (AAU Energy), Aalborg University
9220 Aalborg East, Aalborg, Denmark
[2] College of Electrical Engineering, Zhejiang University
310027 Hangzhou, Zhejiang, China
E-mails: {yuboso, sssa, fbl}@energy.aau.dk, yoy@zju.edu.cn
URL: https://www.energy.aau.dk/

Acknowledgements

The work is supported by the REliable Power Electronic-Based Power System (REPEPS) project at Department of Energy (AAU Energy), Aalborg University, Denmark, as a part of the Villum Investigator Program funded by the Villum Foundation, Denmark.

Keywords

«Microgrid», «Stability», «Reliability», «DC-AC converter», «Capacitors».

Abstract

Stability and reliability are vital performance metrics for microgrid systems, while their interdependency on each other has not been well addressed. This paper thereby explains the relationships between them from a conditional perspective using the Bayesian inference, where the observed stability performance influences the evaluation of system reliability. A DC-AC converter system considering the degradation of filter capacitors is exemplified to illustrate the reliability under stability conditions, with simulation and experimental results provided in order to demonstrate the basic idea.

I. Introduction

Power electronics is the key to power conversion in microgrids, enabling the utilization of renewable energy sources (RES) [1]. However, in such systems, various controllers are leading to heterogeneous dynamics, and mission profiles are bringing about more complexity in the system and stressing the components. Stability and reliability are thereby studied to reduce the abnormalities and/or failures in microgrids.

Stability anticipates the ability of a system to achieve an equilibrium point after being subjected to disturbances, and the dynamic stability is related to the controllers and the system configurations [2], [3]. Microgrid stability is usually modeled by deterministic state-space- or impedance-based approaches [4], [5]. Yet in practice, system uncertainties like the parameter variations or load fluctuations may also lead to an improper design of controllers and system instability [6]. Thus, probabilistic stability is introduced to alternatively describe microgrid performances considering the uncertainties.

Reliability is another index for microgrid performance with a longer timescale. The reliability of power electronics components is related to their degradation, and the mission profiles are playing a critical role in terms of the failure mechanisms [7]. In microgrids, the system-level reliability is characterized based on the functional relationships of the components [8], and the lifetime can be prolonged by, e.g., reliability-oriented control [9], which contributes much to lower the operational cost.

However, the stability and reliability can be closely coupled with each other. For example, component parameters like capacitances may decrease over time [10], and the degradation will affect system stability if the controllers are not updated timely. Under this scenario, conditional probability should be more accurate given a certain system state observability, which is not well addressed in previous literature. Therefore, this paper is aimed at filling this fundamental gap and forming an understanding of the conditional performance by analyzing the impact of component degradation on system stability and reliability.

In this paper, a mathematical formulation using conditional explanation of stability and reliability is provided, and their probabilistic relationships are interpreted based on Bayesian inference. Case studies have been conducted with simulation and experimental results demonstrating the essence of the proposed framework.

II. Probabilistic Stability and Reliability Evaluation in Microgrids

A grid-forming converter system is exemplified in Fig. 1 to illustrate the idea of this paper, which is typical in AC microgrids. It consists of an *LC* filter, a resistive load and a double-loop proportional-integral (PI) voltage controller. Key parameters of this system are listed in Table I.

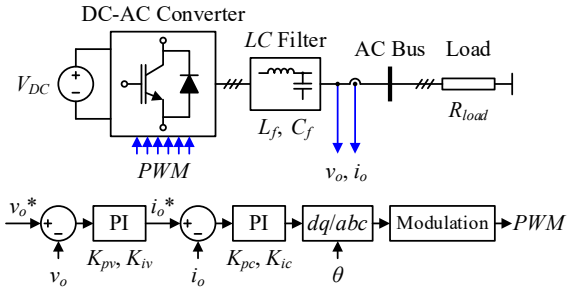

Fig. 1: An exemplary grid-forming converter system with a resistive load. A double-loop voltage controller is employed.

Table I: Key Parameters of the Study Case

Parameters	Values
DC-link voltage V_{DC}	400 V
Rated AC phase voltage V_n	110 V rms
Rated AC frequency f_n	50 Hz
Switching frequency f_{sw}	10 kHz
Resistive load power P_{load}	5 kW
Inductance of the *LC* filter L_f	2.0 mH
Capacitance of the *LC* filter C_f	15 μF
Parameters of voltage controller	K_{pv} = 0.04
	K_{iv} = 78
Parameters of current controller	K_{pi} = 10.5
	K_{ic} = 16000

A. Probabilistic Stability Evaluation

Stability in microgrids can be basically classified into dynamic stability, transient stability and steady-state stability [2]. In this paper, the small-signal dynamic stability is the major focus, which is commonly seen in microgrids. It is normally related to system configurations and controllers, and it can be characterized by state-space- or impedance-based approaches in the frequency domain.

In this case, the system can be modeled into a closed-loop transfer function as:

$$G_{sys}(s) = \frac{V_o(s)}{V_o^*(s)} \tag{1}$$

where, V_o*(s) and V_o(s) are the Laplacian forms of v_o* and v_o in the frequency domain, respectively. With this, the stability of the system can be determined by plotting the root loci of G_{sys} and identify the right-half-plane (RHP) poles (especially the critical modes). For more general cases with multiple converters, the stability can be characterized by plotting the eigenvalue loci of the state matrix as well.

In microgrids, the stability may also vary unexpectedly due to uncertainties. Typical uncertainties include internal configuration uncertainties (like the errors of parameters) and external mission profiles / disturbance events (like ambient temperature, wind speed or solar irradiance) [6]. Among these uncertainties, the parameter uncertainties of components are studied in this paper, which can normally be described by a Gaussian distribution with the Probability Density Function (PDF) as:

$$f(X) = \frac{1}{\sigma\sqrt{2\pi}} \cdot \exp\left[-\frac{1}{2}\cdot\left(\frac{X-\mu}{\sigma}\right)^2\right] \tag{2}$$

where, X is a certain parameter of a component like the inductances, capacitances or parasitic resistances, and μ and σ are its mean value and standard deviation, respectively.

By identifying the distribution of the poles (imaginary part) of G_{sys} specified in (1), the stability of the system will be a probabilistic event, namely the probabilistic distribution of stability.

B. Probabilistic Reliability Evaluation

The reliability, on the other hand, is a longer-term performance index for microgrids, which is normally related to the degradation of components. As power semiconductors and capacitors are among the most fragile components in power electronics, their lifetime models are introduced below.

One of the commonly used models for power semiconductors is the cycle-based lifetime model [11]. The lifetime is measured by a number of power cycles N_f, which is formulated as:

$$N_f = A \cdot \Delta T_j^{\alpha} \cdot \exp\left(\frac{\beta_1}{T_{jm}}\right) \cdot t_{on}^{\gamma} \tag{3}$$

where, the average junction temperature T_{jm} and the junction temperature swing ΔT_j are the major factors, while A, α, β_1 and γ are the coefficients fit from power-cycling tests.

The lifetime of capacitors can be calculated based on the hot-spot temperature and voltage of operation [12], given as:

$$L = L_0 \cdot 2^{\frac{T_0 - T}{n_1}} \cdot \left(\frac{V}{V_0}\right)^{-n_2} \tag{4}$$

where, L_0 is the rated lifetime when operating at the nominal voltage V_0 and temperature T_0. Here, n_1 and n_2 are also constant coefficients.

With this, the accumulated damage D can be calculated according to the Miner's rule [12]:

$$D_{sw} = \sum_i \frac{n^{(i)}}{N_f^{(i)}} \text{ or } D_{cap} = \sum_i \frac{\Delta t^{(i)}}{L^{(i)}} \tag{5}$$

The accumulated damage in (5) is a normalized value, which is, by the end-of-life (EOL) of a component, its damage D should be accumulated to 1. It should be noticed that the lifetime derived from (3)-(5) is statistically the B_{10} lifetime, i.e., when 10% of the device population will statistically fail.

The time-to-failure data of the components follow the Weibull distribution. Accordingly, the probabilistic reliability can be fitted as:

$$R(t) = \exp\left[-\left(\frac{t}{\eta}\right)^{\beta}\right] \tag{6}$$

where, β is the shaping factor, and η is the characteristic lifetime. The B_{10} lifetime can be applied here with R equal to 90%.

Moreover, if all components are supposed to be functioning and no redundancy is considered, the reliability of the system is the multiplication of the reliability of the components, which is then the system-level reliability.

III. Bayesian Mapping of Probabilistic Stability and Reliability in Microgrids

A. The Bayes' Theorem

The Bayes' theorem is a basis in probability theory, which describes the probability of an event with the prior knowledge under a certain condition. It is mathematically expressed as:

$$P(A \mid B) = \frac{P(B \mid A)P(A)}{P(B)} \tag{7}$$

where, A and B are two probabilistic events, and $P(A|B)$ is the conditional probability of the event that A occurs given that B is true. The above equation is basically derived from the calculation of conditional probability, namely:

$$P(A \mid B)P(B) = P(B \mid A)P(A) = P(A \cap B) \tag{8}$$

where, $P(A \cap B)$ is the probability that both two events A and B occur simultaneously. If A and B are probabilistically independent events, the following equations consequently hold:

$$\begin{cases} P(A \cap B) = P(A)P(B) \\ P(A \mid B) = P(A) \\ P(B \mid A) = P(B) \end{cases} \tag{9}$$

One of the most important applications of the Bayes' theorem is the Bayesian inference, which is often applied in data science and information technology, as shown in (10):

$$P(H \mid E) = \frac{P(E \mid H)P(H)}{P(E)} \tag{10}$$

where, the posterior probability $P(H|E)$ of a hypothesis H given the obtained data E can be calculated out of the prior probability $P(H)$ of the hypothesis and the likelihood $P(E|H)$ of the data under the hypothesis.

B. A Bayesian Mapping of the Conditional Probability of Stability and Reliability

For microgrids, stability and reliability are performance indices seen from different

perspectives and in different timescales, and their joint probabilities can be summarized as Table II. A microgrid can be reliable when instability occurs due to parameter mismatch, while it can also be operating stably when one or more components or converters become worn out and are disconnected from the system. Generally, $P(S)$ and $P(R)$ in Table II can be calculated based on the modeling approaches mentioned in Section II, where stability and reliability are considered separately. However, microgrids are supposed to operate both stably and reliably, or in other words, the probability $P(S \cap R)$ should be sufficiently high.

Table II: Joint Probabilities of Stability and Reliability in Microgrids

	Stable	**Unstable**	**Sum**
Reliable	Stable and Reliable $P(S \cap R)$	Reliable but Unstable $P(\neg S \cap R)$	$P(R)$
Unreliable	Stable but Unreliable $P(S \cap \neg R)$	Unreliable and Unstable $P(\neg S \cap \neg R)$	$1-P(R)$
Sum	$P(S)$	$1-P(S)$	1

*Note: S and R are used for denoting the events *stability* and *reliability*, respectively.

As reliability is a performance index in a longer timescale than stability, their joint probability basically reflects the system states in shorter time frames decomposed from the entire timespan under study. Considering the Bayesian inference (10), $P(S|R)$ can thereby be mapped as the likelihood of stability if all components are within their lifetime, and the conditional probability $P(R|S)$ is the posterior probability of reliability.

Accordingly, the reliability under stability conditions can be concluded as:

$$P(R \mid S) = \frac{P(S \mid R) P(R)}{P(S)} \tag{11}$$

where, $P(R|S)$ can be interpreted as an estimation of future reliability given that the system is stable for the time being. This index is more practical, reflecting the long-term performances based on the observed short-term system states.

Specifically, if the stability and reliability are mathematically independent events, then the conditional probability will be given as:

$$\begin{cases} P(S \cap R) = P(S) P(R) \\ P(R \mid S) = P(R) \\ P(S \mid R) = P(S) \end{cases} \tag{12}$$

which just corresponds to an individual analysis on the stability or reliability of the microgrid.

IV. Case Study

The microgrid shown in Fig. 1 is selected as the study case, where the impact of filter capacitor degradation on system stability and reliability is studied. The reliability under stability conditions is derived based on the Bayesian inference to illustrate the aforementioned mapping relationship.

In this case, to simplify the analysis, it is assumed that the filter capacitance C_f is the only variable considered in the stability and reliability analysis, and the three phases are always balanced with the same filter capacitance C_f. Under this scenario, the probabilities of stability and reliability in a three-phase system will be equal to those of a single capacitor.

A. Stability Analysis

Now that the closed-loop transfer function can be constructed as (1), the root loci with respect to the variation of C_f can be plotted as shown in Fig. 2, where only the poles most closed to the imaginary axis (critical modes) are considered. The decrease of the capacitance C_f is equivalent to an increase in the voltage PI gains K_{Pv} and K_{iv}, which leads to an instability in the system.

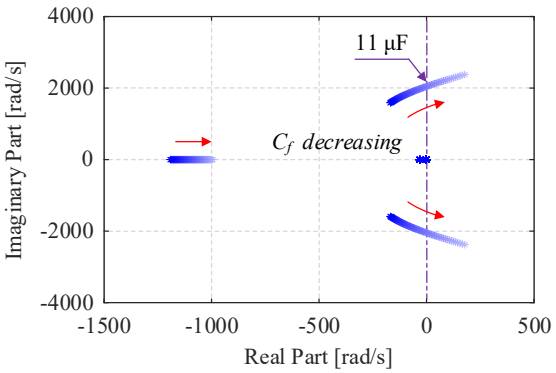

Fig. 2: Root loci of the converter system when the filter capacitance C_f decreases. Only the critical modes are considered in this figure.

The stability performance can also be illustrated by Fig. 3. The filter capacitance is decreased from 15 μF to 10 μF, and in Fig. 3(b), the waveforms showing serious distortions with harmonics indicate that the decrease of capacitance will cause instability. As the capacitance varies due to degradation (which will be elaborated in the next section), the probability of system stability will thereby be influenced.

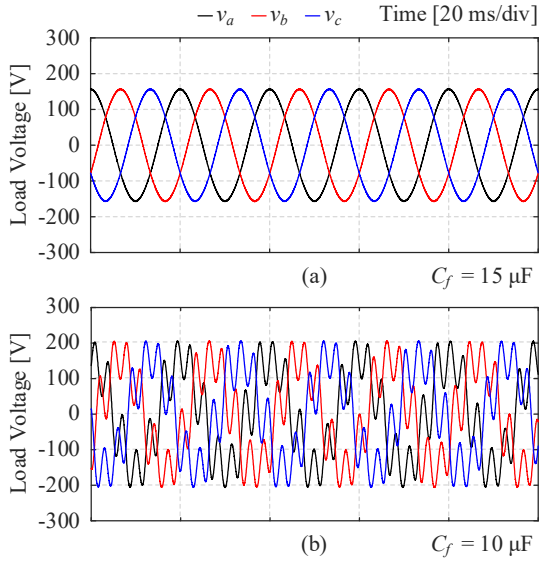

Fig. 3: Load voltage waveforms: (a) C_f = 15 μF, and (b) C_f = 10 μF. The system becomes unstable when the capacitance C_f decreases.

B. Reliability Analysis

For reliability analysis, the AC filter capacitors C_f are selected as Metallized Polypropylene Film Capacitors (MPPF-Caps), of which the constant n_2 in (4) is around 7~10 [12] and selected to be 7 in this study. The type of the capacitors is selected to be the R75H series of KEMET, of which the key parameters are listed in Table III.

Table III: Rated Parameters of the Capacitors

Parameters	Values
Rated lifetime[1] of the capacitor	1000 h
Rated AC voltage of the capacitor	160 V
Uncertainty of the capacitance[2]	±10%

*Note 1: The rated lifetime in the datasheet is regarded as B_{20} lifetime according to [8], which can be converted to B_{10} lifetime like Fig. 4.
*Note 2: The uncertainty is empirically assumed to be the 3σ region in statistics as [14].

According to [10], the capacitance of capacitors will decrease over usage time due to degradation, which can be expressed as:

$$C_t = C_0 \cdot (1 - \alpha \cdot t),\ \alpha > 0 \tag{13}$$

where, C_t denotes the capacitance at usage time t.

Similar to [8], the capacitors are also assumed to be worn out when there is a capacitance drop as much as 20% of the initial value, namely $C_t < 80\%C_0$. If the capacitance follows the Gaussian distribution specified in (2), the reliability should be evaluated by calculating the value of the Cumulative Density Function (CDF) as time goes on, namely F ($0.8C_0$) with the mean value C_t. Thus, the reliability curve can be plotted, as shown in Fig. 4, with the B_{10} lifetime acquired as 9178 h given 110-V AC voltage.

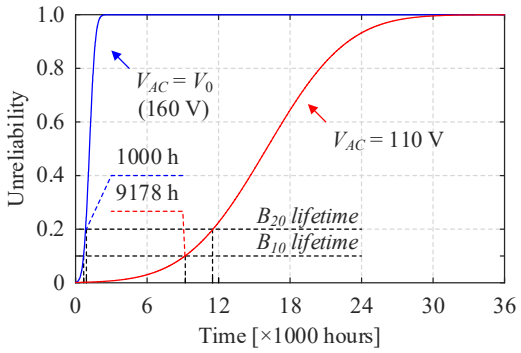

Fig. 4: System unreliability influenced by capacitor degradation. The rated AC voltage of the selected capacitor is 160 V, while the case is studied under 110-V AC voltage according to Table I.

C. Reliability under Stability Conditions Based on the Bayesian Inference

Considering both aspects, the stable and reliable region of the system with respect to the filter capacitance can be illustrated in Fig. 5. The degradation of the capacitors corresponds to the decrease of the mean value of the probability density curve. Considering the unstable and unreliable regions as modeled in the previous section, the probabilities of stability and reliability satisfy:

$$\begin{cases} P(S) = P(C \geq C_S)\big|_t \\ P(R) = P(C \geq C_R)\big|_t \end{cases} \tag{14}$$

where, C_S and C_R are the minimum allowed capacitance that can ensure the system stability and reliability, respectively.

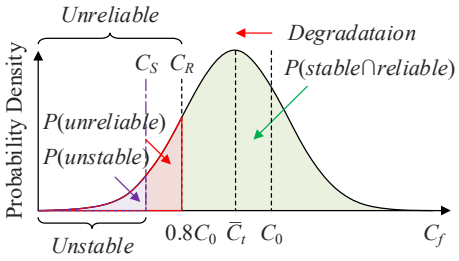

Fig. 5: Illustration on the stable and reliable region in terms of the probabilistic distribution of filter capacitance.

As specified previously, the reliability boundary C_R is 80%C_0, or 12 μF, while the stability boundary is selected as 11.5 μF in order to reserve some stability margin compared to the borderline in Fig. 2. With this, the probability of stability, given that the system is reliable, should be:

$$P(S \mid R) = \frac{P(C \geq C_S)}{P(C \geq C_R)}\bigg|_t = 1 \qquad (15)$$

The degradation of the filter capacitance over time is accordingly presented in Fig. 6, considering the region where the system operates stably. The probability density curve moves leftwards from the initial capacitance, and both $P(S)$ and $P(R)$ decrease over time. The B_{10} lifetime is reached when the cumulated probability F ($0.8C_0$) equals 10%, and the mean capacitance is denoted as C_1 in Fig. 6.

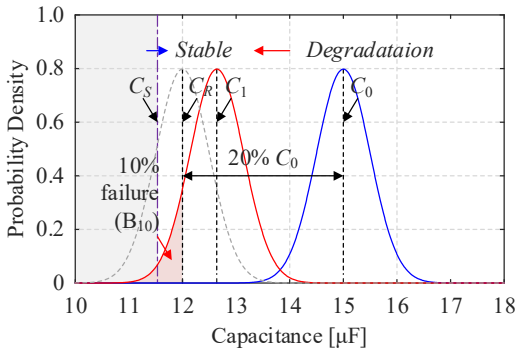

Fig. 6: Degradation of filter capacitance over time.

If the system stability is already observed, then the posterior reliability can be analyzed using the Bayesian inference. The results of unconditional and conditional reliability analysis are compared in Fig. 7. In this case, if the system is stable, then the posterior unreliability should be lower than that without state observation, indicating that the lifetime expectation can actually be longer. The Bayesian framework can thereby be instructive for a better scheduling of maintenance in practice.

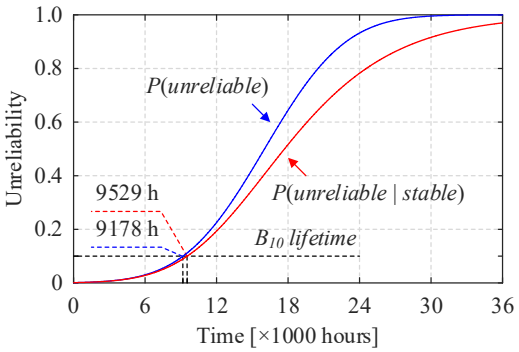

Fig. 7: Comparison of unconditional and conditional reliability analysis on the study case.

Besides, the difference between unconditional and conditional reliability analysis will be more significant when the capacitors are approaching their EOL. The capacitance drops as time goes on, and the probability of stability consequently decreases, which, according to (11), leads to the deviation of $P(R|S)$ from $P(R)$. Cases are similar when, e.g., the parameters have large uncertainty, or the system is designed to operate closer to its stability boundary. This could also reflect the probabilistic interactions between system-level stability and reliability.

V. Experimental Results

The experimental platform is shown in Fig. 8, consisting of DC-AC converter racks, a power amplifier as a voltage source, filters and load resistors. Two three-phase Silicon-Carbide (SiC) converters are installed inside each rack with the rated power being 10 kW. To demonstrate the study case, the platform is configured in similar structure as shown in Fig. 1, utilizing a second DC-AC converter to establish the DC-link. In experimental tests, the load resistor is downscaled to 80 Ω (0.5 kW) due to available hardware components. The control parameters are also appropriately adjusted based on Table I to account for the disparities in parasitic parameters between simulations and experimental tests.

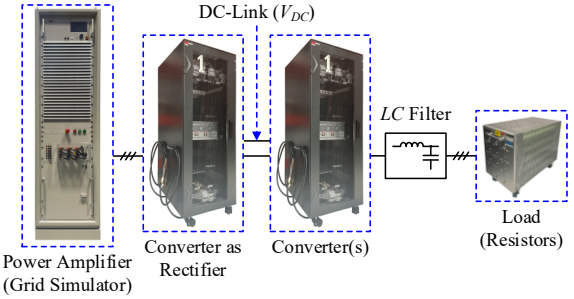

Fig. 8: Hardware platform to facilitate the experimental tests, which is configured based on the exemplary system in Fig. 1.

The results obtained on this platform are presented in Fig. 9, demonstrating the influence of filter capacitance variations. By comparing the subfigures (a) and (b), it is revealed that the decrease in C_f from 15 μF to 10 μF can result in impaired system stability, which can be a system-level side-effect of capacitor degradation. Thus, it is of great significance to incorporate stability considerations when evaluating system reliability in similar scenarios.

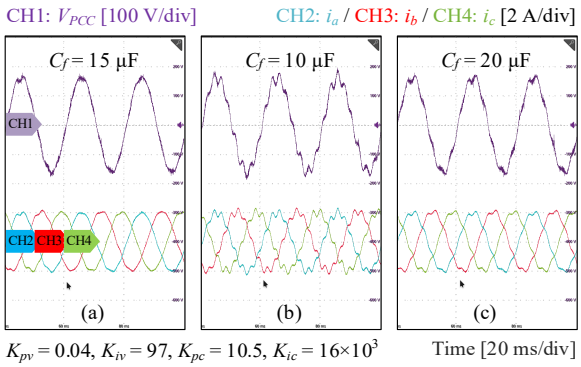

Fig. 9: Experimental results when the filter capacitance C_f varies, (a) C_f = 15 μF, (b) C_f = 10 μF, and (c) C_f = 20 μF.

Besides, when the filter capacitance is increased to 20 μF in Fig. 9 (c), the system approaches instability as well. This stems from the deviation of experimental and simulation configurations, where other approximated factors like the control delays may also influence the root loci of the system. Nevertheless, it is also indicating the impact of more general uncertainties on system performances, which agrees with the stability concerns highlighted in [14]. This concern can be further inspected by data-based methodologies in order to achieve more genuine evaluation of system performances, e.g., condition monitoring for calibrating system states, or artificial-intelligence (AI) based modeling which can better accord with the observed system behaviors.

VI. Conclusion

In this paper, a Bayesian interpretation of the relationships between stability and reliability in microgrids is proposed. The significance of conditional reliability is demonstrated through a case study where the degradation of capacitors affects both stability and reliability. The coupling of stability and reliability is revealed, and this approach can be more practical given that the system performance is observed. The case study has also been illustrated by experimental results when the filter capacitor varies.

In the future, the scope of this paper can be further extended to data-based methodologies for system-level risk evaluation and state prediction, like condition monitoring or AI-based tools using the Bayesian inference, so as to achieve more genuine performance evaluation with the help of system observations.

References

[1] D. Boroyevich, I. Cvetković, D. Dong, R. Burgos, F. F. Wang, and F. C. Lee, "Future Electronic Power Distribution Systems - A Contemplative View," in *Proc. OPTIM 2010*, Brasov, Romania, May 2010, pp. 1369-1380.

[2] M. Farrokhabadi, C. A. Canizares, J. W. Simpson-Porco, E. Nasr, L. Fan, P. A. Mendoza-Araya, R. Tonkoski, U. Tamrakar, N. Hatziargyriou, D. Lagos, R. W. Wies, M. Paolone, M. Liserre, L. Meegahapola, M. Kabalan, A. H. Hajimiragha, D. Peralta, M. A. Elizondo, K. P. Schneider, F. K. Tuffner, and J. Reilly, "Microgrid Stability Definitions, Analysis, and Examples," *IEEE Trans. Power Syst.*, vol. 35, no. 1, pp. 13-29, Jan. 2020.

[3] Y. Song, S. Sahoo, Y. Yang, and F. Blaabjerg, "System-Level Stability of the CIGRE Low Voltage Benchmark System: Definitions and Extrapolations," in *Proc. 2021 IEEE COMPEL*, Cartagena, Colombia, Nov. 2021, pp. 1-6.

[4] N. Pogaku, M. Prodanovic, and T. C. Green, "Modeling, Analysis and Testing of Autonomous Operation of an Inverter-Based Microgrid," *IEEE Trans. Power Electron.*, vol. 22, no. 2, pp. 613-625, Mar. 2007.

[5] J. Sun, "Impedance-Based Stability Criterion for Grid-Connected Inverters," *IEEE Trans. Power Electron.*, vol. 26, no. 11, pp. 3075-3078, Nov. 2011.

[6] K. N. Hasan, R. Preece, and J. V. Milanovic, "Existing Approaches and Trends in Uncertainty Modelling and Probabilistic Stability Analysis of Power Systems with Renewable Generation," *Renewable Sustainable Energy Rev.*, vol. 101, pp. 168-180, Mar. 2019.

[7] H. Wang, M. Liserre, F. Blaabjerg, P. d. P. Rimmen, J. B. Jacobsen, T. Kvisgaard, and J. Landkildehus, "Transitioning to Physics-of-Failure as a Reliability Driver in Power Electronics," *IEEE J. Emerging Sel. Top. Power Electron.*, vol. 2, no. 1, pp. 97-114, Mar. 2014.

[8] D. Zhou, H. Wang, and F. Blaabjerg, "Mission Profile Based System-Level Reliability Analysis of DC/DC Converters for a Backup Power Application," *IEEE Trans. Power Electron.*, vol. 33, no. 9, pp. 8030-8039, Sept. 2018.

[9] Y. Song, S. Sahoo, Y. Yang, and F. Blaabjerg, "Conditional Droop Adjustment for Reliability-

Oriented Power Sharing in Microgrids," *IEEE Trans. Circuits Syst. II Express Briefs*, vol. 70, no. 7, pp. 2465-2469, Jul. 2023.

[10] B. Sun, X. Fan, C. Qian, and G. Zhang, "PoF-Simulation-Assisted Reliability Prediction for Electrolytic Capacitor in LED Drivers," *IEEE Trans. Ind. Electron.*, vol. 63, no. 11, pp. 6726-6735, Nov 2016.

[11] R. Bayerer, T. Herrmann, T. Licht, J. Lutz, and M. Feller, "Model for Power Cycling Lifetime of IGBT Modules – Various Factors Influencing Lifetime," in *Proc. 5th International Conference on Integrated Power Electronics Systems*, Nuremberg, Germany, Mar. 2008, pp. 1-6.

[12] H. Wang and F. Blaabjerg, "Reliability of Capacitors for DC-Link Applications in Power Electronic Converters - An Overview," *IEEE Trans. Ind. Appl.*, vol. 50, no. 5, pp. 3569-3578, Sep.-Oct. 2014.

[13] M. A. Miner, "Cumulative Damage in Fatigue," *J. Appl. Mech.*, vol. 12, no. 3, pp. A159-A164, 1945.

[14] Y. Song, S. Sahoo, Y. Yang, and F. Blaabjerg, "Probabilistic Risk Evaluation of Microgrids Considering Stability and Reliability," *IEEE Trans. Power Electron.*, vol. 38, no. 8, pp. 10302-10312, Aug. 2023.